

**United States
Department of
Agriculture**

**Natural Resources
Conservation
Service**

**11 Campus Boulevard,
Suite 200
Newtown Square, PA 19073**

Subject: SOI – Geophysical Field Assistance

Date: 15 February 2006

To: Dr. Henry Lin

Assistant Professor of Hydropedology/Soil Hydrology
Crop & Soil Sciences Department
415 Agricultural Sciences and Industries Building
Pennsylvania State University
University Park, PA 16802

Edward White
State Soil Scientist
USDA-NRCS
One Credit Union Place, Suite 340
Harrisburg, PA 17110-2993

Purpose:

Ground-penetrating radar (GPR) was used to characterize limestone bedrock in an area of Opequon soil.

Activities:

This assignment was completed on 20 January 2006.

Participants:

Jim Doolittle, Research Soil Scientist, USDA-NRCS-NSSC, Newtown Square, PA

Mike Mcdevitt, Soil Scientist, USDA-NRCS, Mill Hall, PA

Yuri Plowden, Soil Scientist, USDA-NRCS, Mill Hall, PA

Bob Zhou, Postdoctoral Research Associate, Department of Crop and Soil Sciences, Pennsylvania State University, University Park, PA

Shujiang Kang, Candidate, PhD in Soil Science, Department of Crop and Soil Sciences, Pennsylvania State University, University Park, PA

Summary:

This exercise was conducted to help emphasize a possible role of GPR in hydropedological investigations and the need to better understand and characterize the underlying bedrock. While the use of GPR is highly site-specific and similar results cannot be obtained over most soils, the use of GPR in hydropedological investigations should be at least considered.

It was my pleasure to participate in this study and to work with Yuri, Mike, and the graduate students of Pennsylvania State University.

With kind regards,

James A. Doolittle
Research Soil Scientist
National Soil Survey Center

cc:

B. Ahrens, Director, National Soil Survey Center, USDA-NRCS, Federal Building, Room 152, 100 Centennial Mall North, Lincoln, NE 68508-3866

- S. Carpenter, MLRA Office Leader, USDA-NRCS, 75 High Street, Room 301, Morgantown, WV 26505
- M. Golden, Director, Soil Survey Division, USDA-NRCS, Room 4250 South Building, 14th & Independence Ave. SW, Washington, DC 20250
- D. Hammer, National Leader, Soil Survey Investigations, National Soil Survey Center, USDA-NRCS, Federal Building, Room 152, 100 Centennial Mall North, Lincoln, NE 68508-3866
- W. Tuttle, Soil Scientist (Geophysical), National Soil Survey Center, USDA-NRCS, P.O. Box 60, 207 West Main Street, Rm. G-08, Federal Building, Wilkesboro, NC 28697

Background:

The depth, topography, and structure of bedrock influence the flow of water. Bedrock restricts, redirects, and concentrates the flow of water. As restrictive layers, lithic and paralithic contacts promote lateral flow, and discontinuities (joints, fractures, and sedimentary layering) foster preferential flow through bedrock. Joints and fractures create additional permeability across lithologic boundaries. The amount of water that flows through these discontinuities is influenced by their size, orientation, spacing, persistence, and filling materials. Saturated conditions frequently develop above some soil-bedrock interfaces. The presence of depressions in these bedrock surfaces aggravates the development and persistence of saturated conditions, which influences the development of redoximorphic features in soils. Bedrock lips punctuate and divide the apparent water table into zones, which interrupt groundwater flow towards the riparian zone (Buttle et al., 2004).

Variable soil thickness or depths to bedrock exerts a considerable control on the ability of slope elements to deliver runoff to riparian zones and should be considered in all monitoring and modeling projects (Buttle et al., 2004). Many hydrological models assume that the surface and bedrock slopes mirror one another; an assumption that reflects the lack of adequate observations on the spatial variability of soil depth (Buttle et al., 2004). The shape of the bedrock surface control subsurface flow patterns more than the shape of the surface slope (Beven, 2001). Hydrologic models such as TOPMODEL assume that soil thickness is uniform throughout the drainage basin and that the hydraulic gradient of the saturated zone approximates the surface slope (Wolock, 1993). At smaller scales, these assumptions are incorrect; at larger scales, these assumptions are oversimplifications that weaken the accuracy of results (Lin et al., 2005).

Hydropedological investigations should extend through whatever materials and depths necessary to satisfy research objectives (Lin et al., 2005). In many upland areas, in order to better understand the flow of water through the vadose zone, hydropedological investigations need to extend into the upper portions of the underlying bedrock. Viewing, let alone characterizing, the underlying bedrock is difficult and impractical in most situations, and is often limited to a restrictive number of outcrops, exposures, or core site. In the absence of continuous and satisfactory outcrops or exposures, ground-penetrating radar (GPR) is an accepted tool for imaging the subsurface in many hydrogeologic studies (Beres and Haeni, 1991).

Use of Ground-penetrating radar in bedrock investigations:

Ground penetrating radar has been used extensively to chart bedrock depths (Collins et al., 1989; Davis and Annan, 1989), changes in rock type (Davis and Annan, 1989), characterize fractures and joint patterns (Porsani et al., 2005; Nascimento da Silva et al., 2004; Lane et al., 2000; Pipan et al., 2000; Grasmueck, 1996; Stevens et al., 1995; Toshioka et al., 1995; and Holloway and Mugford, 1990), cavities, sinkholes, and fractures in limestone (Al-fares et al., 2002; Pipan et al., 2000; Barr, 1993) and faults (Demanet et al., 2001; Meschede et al., 1997). In mining and quarry operations, GPR has been used to detect geologic hazards and to optimize extraction costs (Singh and Chauhan, 2002; Grodner, 2001; and Molinda et al., 1996).

Ground-penetrating radar has been used in hydrogeologic investigations to study the structure (fractures, unloading or exfoliation joints, bedding and stress planes, cavities, etc.) of the underlying bedrock (Porsani et al., 2005; Al-fares et al., 2002; Singh and Chauhan, 2002; Beres and Haeni, 1991). In limestone, seepage is more likely to occur in those portions that are karstified and contained extensive fractures and cavities. Ground-penetrating radar has revealed structural features (e.g., bedding and fracture planes, karstified zones, compacted and massive limestone, and conduits) in limestone, which influenced the infiltration of water (Al-fares et al., 2002).

Study Site:

This study was conducted in central Pennsylvania in the Valley and Ridge structural province. The study site is located in Ferguson Township, Centre County. The approximate location of the study site is 40.70483° N Lat. and 77.96592° W Long. The approximate location of the detailed grid survey is identified by a small red-colored box on the soil map shown in Figure 1. The grid site is located in an area of Opequon-Hagerstown complex, 3 to 8 percent slopes (OhB), but closely borders a miscellaneous area, Quarry (Qu). The well drained, shallow Opequon and the very deep Hagerstown soils formed in materials weathered from limestone. The Opequon soil is a member of the

clayey, mixed, mesic Lithic Hapludalfs family. The Hagerstown soil is a member of the fine, mixed, mesic Typic Hapludalfs family. The area is underlain by the Coburn formation through the Loysburg formation (undivided Ordovician limestone and calcareous shale).

Materials and Methods:

The radar unit is the TerraSIRch Subsurface Interface Radar (SIR) System-3000 (here after referred to as the SIR System-3000), manufactured by Geophysical Survey Systems, Inc. (North Salem, New Hampshire).¹ The use and operation of GPR is described by Daniels (2004). The SIR System-3000 consists of a digital control unit (DC-3000) with keypad, SVGA video screen, and connector panel. The SIR System-3000 weighs about 4.1 kg (9 lbs) and is backpack portable. With an antenna, this system requires two people to operate. The 200 and 120 MHz antennas were used in this study.

The RADAN for Windows (version 5.0) software program developed by Geophysical Survey Systems, Inc, was used to process all radar records.¹ Processing included setting the initial pulse to time zero, color table and transformation selection, marker editing, distance normalization, range gain adjustments, migration, and surface normalization. All radar records were migrated to remove hyperbola diffractions and to correct the geometry of inclined layers. Surface normalization corrects the radar record for changes in elevation and, in this study, improved interpretations and the association of subsurface reflectors with soils and landscape components.

To expedite GPR field work, two equal length (15-m) and parallel lines were established across a representative summit area of the Opequon-Hagerstown complex, 3 to 8 percent slopes. These two lines were spaced 15-m apart. The two parallel lines defined a 15 m² grid area. Along each line, survey flags were inserted in the ground at intervals of 50 cm. For positional accuracy, GPR traverses were completed along a reference line, which was stretched and sequentially moved between similarly numbered flags on the two parallel grid lines. Pulling the 200 MHz antenna along the reference line that was stretched between similarly numbered flags on the two parallel survey lines completed a GPR traverse. Along the reference line, marks were spaced at 100-cm intervals. As the antenna was towed passed each reference point, a vertical mark was impressed on the radar record. Walking, in a back and forth manner, along the reference line, which was moved sequentially between similarly numbered flags on the two parallel survey lines, completed the detailed GPR grid survey.

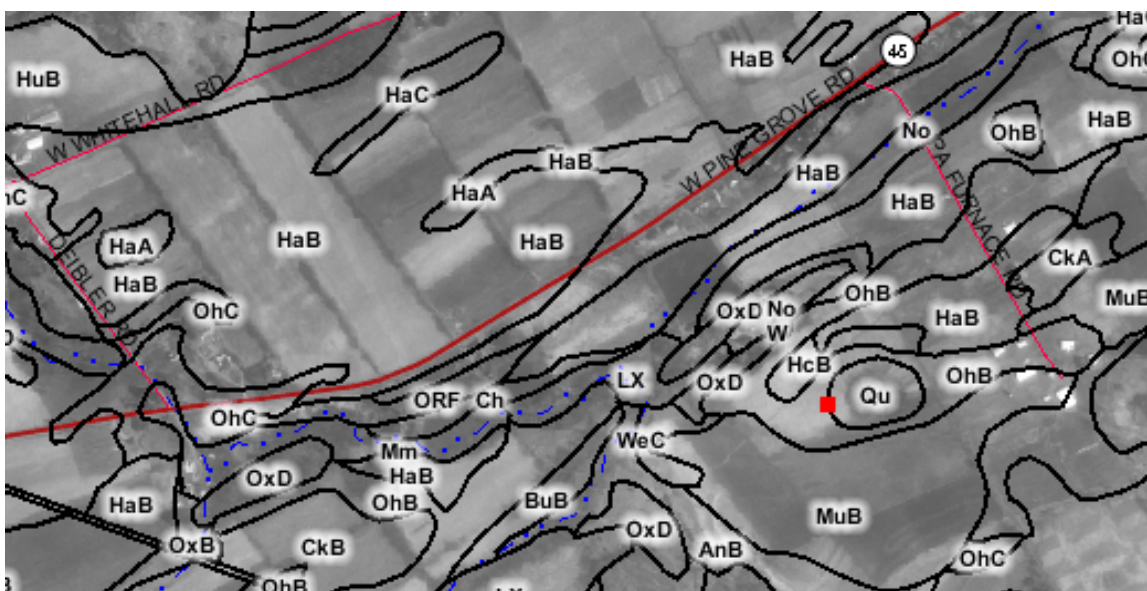


Figure 1. A red square shows the approximate location of the grid site on this soil map from Centre County.

Interpretations:

Figure 2 contains a representative picture and radar record of Opequon soil. Vertical or depth scales are expressed in feet on the soil profile and in meters on the radar record. The radar record has been “surface normalization,” a post-processing procedure that assigns elevations to each reference point so that the radar records can be corrected for changes in surface topography. Surface normalized presentations aid soil/landscape correlations and improves interpretations. In addition, surface normalization contributes to the proper geometric reconstruction of the various structural elements (e.g., discontinuities, bedding and fracture planes) of the underlying bedrock.

Areas of Hagerstown soil are considered poorly suited to GPR. The high clay and moisture contents of Hagerstown soil result in high rates of signal attenuation and restricted penetration depths. In areas of Hagerstown soil, radar penetration depths are restricted to about 1 m. The underlying limestone bedrock is electrically resistive and offers a relatively low energy loss medium to GPR. In areas of Opequon soil, where the electrically resistive limestone occurs at shallow depths, rates of signal attenuation are less and the effective depth of penetration is greater. On the radar record shown in Figure 2, the GPR’s penetration depth exceeds 4 m.

The underlying limestone bedrock is characterized by gently dipping, high amplitude planar reflectors. In rocks, radar reflections result from abrupt changes in lithologic properties (density, porosity, grain size, clay content, etc.) and water content (Corbeau et al., 2001b). Contacts separating different lithologic units are identified by differences in reflected signal amplitudes, termination of reflections, and different reflection patterns (continuity and geometric configurations) (Corbeau et al., 2001b). These features are not evident on the radar record shown in Figure 2.

Abrupt changes in water content do produce high amplitude radar reflections. High amplitude radar reflections are associated with water filled joints, fractures, and structural planes (Lane et al., 2000; Buursink and Lane, 1999; Olhoeft, 1998; Grasmueck, 1994). In Figure 2, the slightly dipping sub-parallel reflectors evident on the radar record represent bedding planes in the limestone. These reflectors vary spatially in form and signal amplitude. Variations in signal amplitudes are attributed principally to differences in moist contents along bedding planes. If moisture flows along these surfaces, the flow is downslope and to the left (south) in Figure 2.

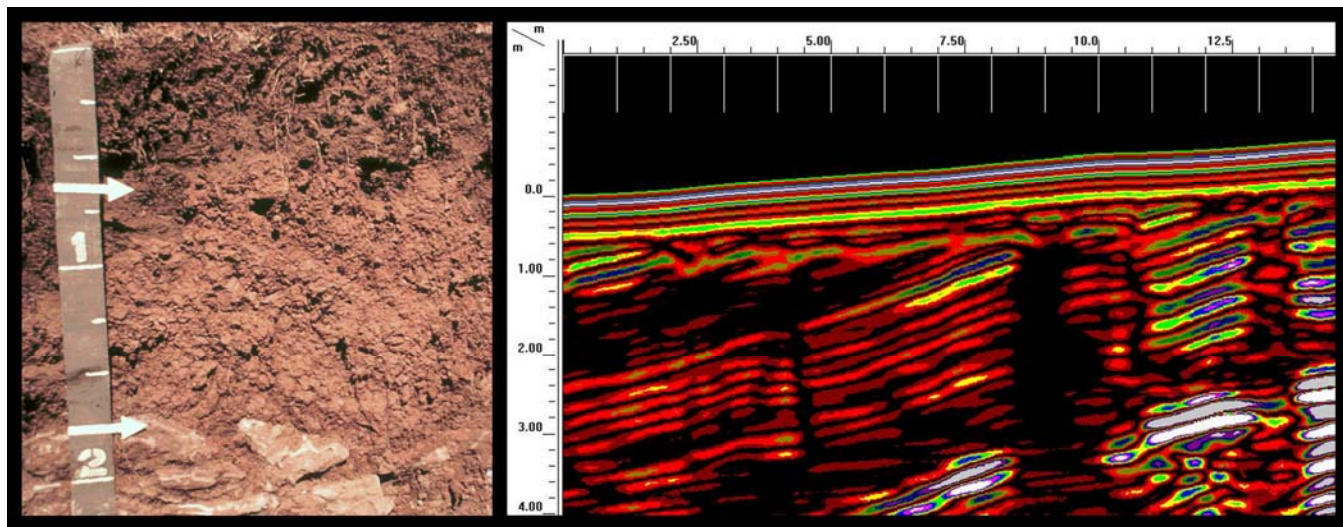


Figure 2. Representative soil profile (left) and radar record (right) of Opequon soil.

Differences in the geometry, separation, and contents of fractures and bedding planes affect detection. Because of scattering losses, attenuation, wave length-scale heterogeneities, and geometric constraints, the number of fractures interpreted on radar records is an order of magnitude less than the number typically observed in outcrops (Lane et al.,

2000). Closely spaced bedding and fracture planes will produce reverberations that masked one another. Fractures spaced closer than $\frac{1}{4}$ of the transmitted wave length are obscured by constructive interference (Lane et al., 2000).

High scattering losses occur in highly fractured rocks and limit the penetration depth and effectiveness of high frequency antennas. For all antennas, scattering losses are greater for reflectors with large dip-angles. These reflectors reflect less energy back to the radar antenna. Fractures and bedding planes with dip-angles greater than about 45° are also affected by spatial aliasing distortion and are not accurately imaged with GPR (Buursink and Lane 1999; Ulriksen, 1982). Spatial aliasing restricts the dip-angles that are detectable with GPR (Lane et al., 2000). Vertical interfaces reflect very little energy towards radar antenna. As a consequence, these reflectors often appear on radar records as numerous low-amplitude diffractions whose alignment reflects the orientation of the steeply inclined fracture (Grasmueck et al., 2004).

Limestone is highly pervious and some water preferentially flows downwards along dipping bedding planes and vertical fractures and joints, which are enlarged by solution. In limestone, circulating water initiates karstification and increases the permeability of rocks. On the radar record shown in Figure 2, noticeable breaks in the gently dipping reflection patterns are evident. These breaks are believed to represent fractures and solution cavities. These fractures and cavities may be filled with soil materials and therefore have higher clay and moisture contents than the surrounding limestone. The higher clay and moisture contents of these features attenuate the radar signal and result in “white-out” areas or areas of no signal return. Not all fractures or solution features are detectable with GPR. Ground-penetrating radar is generally insensitive to fractures with small widths (< 4 mm). Reflection amplitudes increase and waveforms change slightly as fracture width increase from 4 to 16 mm (Lane et al., 2000).

Three-dimensional imagery:

Recent data processing innovations, which allow for the construction of three-dimensional (3D) radar images, have been used to improve the characterization of rock structure and geometry (Grasmueck et al., 2004; Corbeanu et al., 2001b; Szerbiak et al., 2001; Beres et al., 2000; Junck and Jol, 2000; and McMechan et al., 1997). Three-dimensional, radar images can be used to help visualize and describe various structural elements that affect the infiltration and flow of ground water. Three-dimensional radar images have been used to characterize rock features (e.g., inclination, permeable bed elements, and the distribution of flow barriers) that influence the flow of water in sedimentary aquifers (Corbeanu et al., 2001b; Aspron and Aigner, 2000 & 1997).

Full-resolution 3D radar data sets require a dense pattern of very closely spaced, parallel traverse lines (traverse line intervals of 10 to 20 cm are recommended for a 100 MHz antenna) to produce unaliased sampling (Grasmueck et al., 2004). The acquisition of such dense data sets has restricted the wide use of full-resolution 3D radar imaging (Grasmueck et al., 2004). These dense data sets must be appropriately processed. In order to focus energy and correctly orientate inclined reflectors, processing should include 3D depth migration, which allows for a more direct and accurate comparison of geologic and radar data (Corbeanu et al., 2001a). In rugged, topographically diverse terrains, the collection of these dense radar data sets is more complicated and requires the use of nonstandard procedures (Heincke et al., 2005). Because of technical concerns and the unavailability of appropriate and powerful processing software, most 3D radar data sets have been recorded across relatively level surface (Heincke et al., 2005). In topographical diverse terrains, the processing of GPR data remains complicated and requires the use of nonstandard procedures (Heincke et al., 2005).

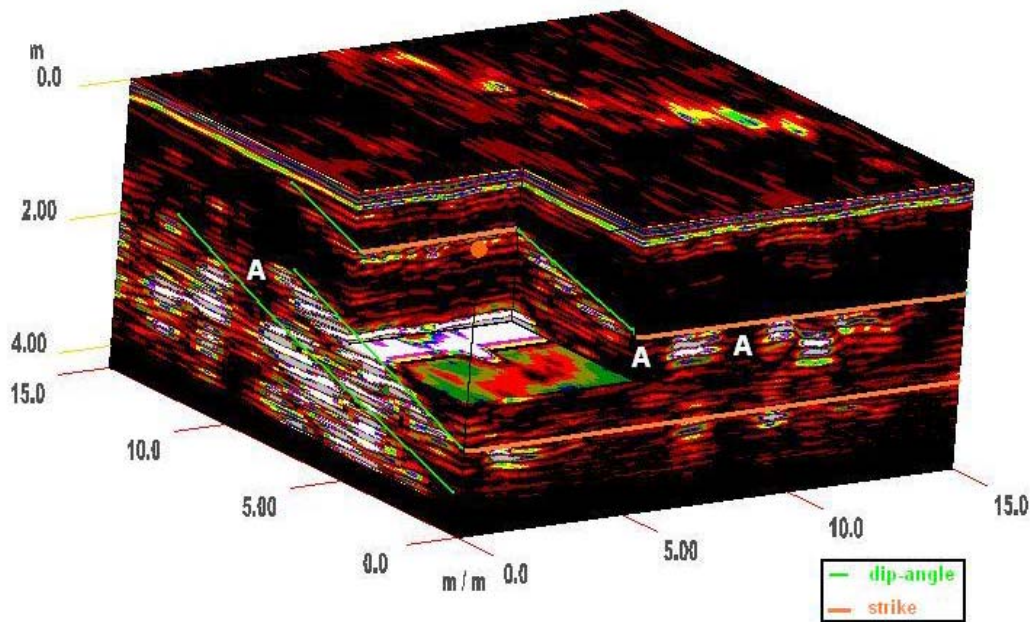


Figure 3. A pseudo-3D image cube display from a GPR grid survey conducted in an area of Opequon soil.

Figure 3 is a 3D cube display of the radar data collected at the survey site. The dimensions of this cube are 15 by 15 by 4.2 m. Radar data were collected along a series of traverse lines that were spaced at 50-cm intervals and parallel to the X-axis. These traverse lines are considered too widely spaced to provide a full-resolution 3D GPR survey with the 200 MHz antenna. Full resolution 3D GPR surveys require a closer traverse spacing (10 to 20 cm). Because a 50-cm interval was used, the radar image is more interpolative than a full-resolution 3D image cube and is therefore considered a “pseudo-3D image cube” (Grasmueck et al., 2004).

In Figure 3, a 5 by 5.2 by 2.3 m cutout cube has been removed from the foreground to better display the geometry of the sedimentary beds. High amplitude (white colored) reflections represent interfaces between contrasting materials. Differences in moisture contents between the bounding limestone and thin bedding planes are believed to be principally responsible for these high amplitude reflections. In Figure 3, the general dip of several high-amplitude bedding planes are indicated with green-colored lines. The apparent strike of these inclined beds is indicated with orange-colored lines. Within the cutout cube, a relatively broad, high-amplitude, linear band is apparent. Because of its gentle dip-angle, this high-amplitude reflection from an inclined bed appears fairly wide in the cutout. Several probable solution cavities (see ‘A’ in Figure 3) have been identified in Figure 3. These cavities are filled with soil materials and have higher clay and moisture contents than the surrounding limestone. The higher clay and moisture contents of these features attenuate the radar signal and result in “white-out” areas.

Figure 4 is another display of the 3D cube image. Figure 4 is an XYZ fence diagram. Slices have been made through the 3D cube image at X = 5 m, Y = 7.25 m, and Z = 3.2 m. In Figure 4, the general dip and strike of several high-amplitude bedding planes are indicated with green-and orange-colored lines, respectfully. Along the strike and dip of these inclined beds, the surface undulates and varies in signal amplitude. These characteristics reflect karstification. In Figure 4, a solution feature is suggested on an x-axis slice at ‘A.’ The expression of two solution cavities in the horizontal plane (z-axis slice) as they cut through gently dipping, high amplitude beds is apparent at locations identified by ‘B’ in Figure 4.

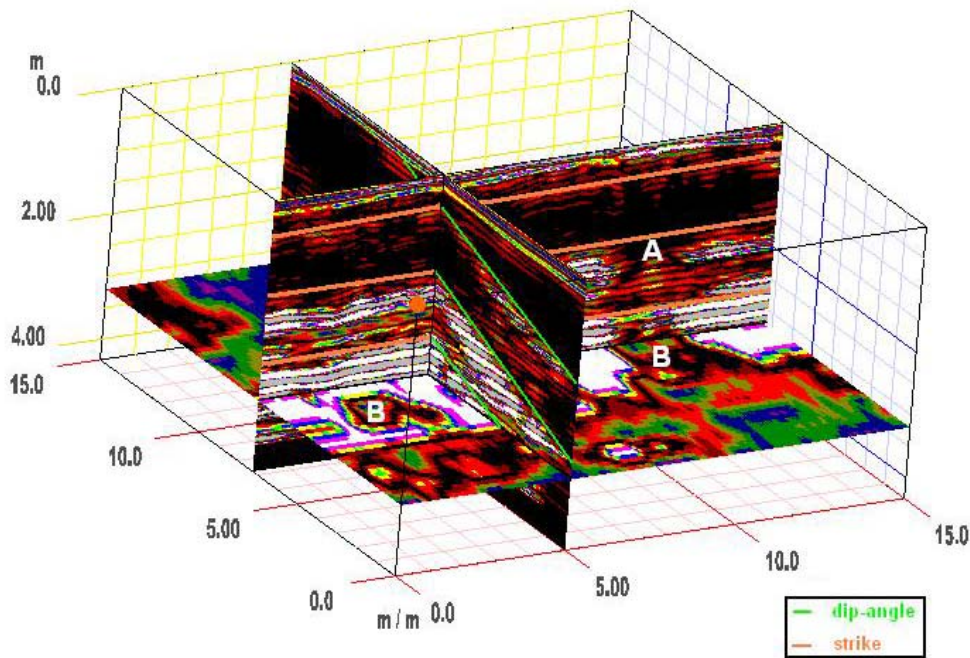


Figure 4. Interpolated fence diagram from the grid area of Opequon soil.

References:

- Al-fares, W., M. Bakalowicz, R. Guerin, M. Dukhan. 2002. Analysis of the karst aquifer structure of the Lamalou area (Herault, France) with ground penetrating radar. *Journal of Applied Geophysics* 51: 97-106.
- Aspiron, U. and T. Aigner. 1997. Aquifer architecture analysis using ground-penetrating radar: Triassic and Quaternary examples (S. Germany). *Environmental Geology* 31: 66-75.
- Aspiron, U. and T. Aigner. 2000. An initial attempt to map carbonate buildups using ground-penetrating radar: an example from the Upper Jurassic of SW Germany. *Facies* 42: 245-152.
- Barr, G. L. 1993. Application of ground-penetrating radar methods in determining hydrogeologic conditions in a karst area, west-central Florida. USGS Water Resources Report 92-4141. Tallahassee, Florida. 26 p.
- Beres, M., A. G. Green, and A. Pugin. 2000. Diapiric origin of the Chessel-Noville Hills of the Rhone Valley interpreted from georadar mapping. *Environmental and Engineering Geoscience*, 6(2): 141-153.
- Beres, M. and F. P. Haeni. 1991. Application of ground-penetrating-radar methods in hydrogeologic studies. *Ground Water* 29(3): 375-386.
- Beven, K. 2001. On hypothesis testing in hydrology. *Hydrological Processes* 15: 1655-1657.
- Buttle, J. M., P. J. Dillon and G. R. Eerkes. 2004. Hydrologic coupling of slopes, riparian zones and streams: an example from the Canadian Shield. *Journal of Hydrology* 287: 161-177.
- Buursink, M.L., and J. W. Lane. 1999. Characterizing fractures in a bedrock outcrop using ground-penetrating radar at Mirror Lake, Grafton County, New Hampshire. 769-776 pp. IN: Morganwalp, D.W., and Buxton, H.T. (eds.), U.S. Geological Survey Toxic Substances Hydrology Program--Proceedings of the Technical Meeting,

- Charleston, South Carolina, March 8-12, 1999--Volume 3 of 3--Subsurface Contamination from Point Sources: U.S. Geological Survey Water-Resources Investigations Report 99-4018C.
- Collins, M. E., J. A. Doolittle, R. V. Rourke. 1989. Mapping depth to bedrock on a glaciated landscape with ground-penetrating radar. *Soil Sci. Soc. Am. J.*, 53(3): 1806-1812.
- Corbeanu, R. M., G. A. McMechan, R. B. Szerbiak, K. Soegaard. 2001a. Prediction of 3-D fluid permeability and mudstone distributions from ground-penetrating radar attributes: Example from the Cretaceous Ferron sandstone member, east-central Utah. *Geophysics* 67(5): 1495-1504.
- Corbeanu, R. M., K. Soegaard, R. B. Szerbiak, J. B. Thurmond, G. A. McMechan, D. Wang, S. Snelgrove, C. B. Forster, and A. Menitove. 2001b. Detailed internal architecture of fluvial channel sandstone determined from outcrop, cores and 3-D ground-penetrating radar: Example from the middle Cretaceous Ferron sandstone, east-central Utah. *American Association of Petroleum Geologists Bulletin* 85(9) 1583-1608.
- Daniels, D. J. 2004. *Ground Penetrating Radar*; 2nd Edition. The Institute of Electrical Engineers, London, United Kingdom.
- Davis, J. L., and A. P. Annan. 1989. Ground-penetrating radar for high-resolution mapping of soil and rock stratigraphy. *Geophysical Prospecting*, 37: 531-551.
- Demagnet, D., L. G. Evers, H. Teerlynck, B. Dost, and D. Jongmans. 2001. Geophysical investigations across the Peel boundary fault (The Netherlands) for a paleoseismological study. *Netherlands Journal of Geosciences* 80 (3-4): 119-127.
- Grodner, M. 2001. Using ground penetrating radar to quantify changes in fracture pattern associated with a simulated rockburst experiment. *Journal of the South African Institute of Mining and Metallurgy*. Vol. 101(5): 261-266.
- Grasmueck, M. 1994. Application of seismic processing techniques to discontinuity mapping with ground-penetrating radar in crystalline rock of the Gotthard Massif, Switzerland. 1135-1149 pp. In *Proceeding of the Fifth International Conference on Ground Penetrating Radar*. Waterloo Centre for Groundwater Research and Canadian Geotechnical Society. June 12-16 1994, Kitchner, Ontario, Canada.
- Grasmueck, M., 1996, 3-D ground-penetrating radar applied to fracture imaging in gneiss: *Geophysics*, v. 61, no. 4, p. 1050-1064.
- Grasmueck, M., R. Weger, and H. Horstmeyer. 2004. Three-dimensional ground-penetrating radar imaging of sedimentary structures, fractures, and archaeological features at submeter resolution. *Geology* 32(11): 933-936.
- Heincke, B., A. G. Green, J. van der Kruk, and H. Horstmeyer. 2005. Acquisition and processing strategies for 3D georadar surveying a region characterized by rugged topography. *Geophysics* 70(6): K53-K61.
- Holloway, A. L., and J. C. Mugford. 1990. Fracture characterization in granite using ground probing radar. *CIM Bulletin* 83 (940): 61- 70.
- Junck, M. B. and H. M. Jol. 2000. Three-dimensional investigation of geomorphic environments using ground penetrating radar. 314-318 pp. IN: (Noon, D. Ed.) *Proceedings Eight International Conference on Ground-Penetrating Radar*. May 23 to 26, 2000, Goldcoast, Queensland, Australia. The University of Queensland.
- Lane Jr., J. W., M. L. Buursink, F. P. Haeni, and R. J. Versteeg. 2000. Evaluation of ground-penetrating radar to detect free-phase hydrocarbons in fractured rocks – results of numerical modeling and physical experiments. *Ground Water*, 38(6): 929-938.

- Lin, H., J. Bouma, L. P. Wilding, J. L. Richardson, M. Kutilek, and D. R. Nielsen. 2005. Advances in hydrogeology. *Advances in Agronomy* 85: 1-75.
- McMechan, G. A., G. C. Gaynor, and R. B. Szerbiak. 1997. Use of ground-penetrating radar for 3-D sedimentological characterization of clastic reservoir analogs. *Geophysics*, 62(3): 786-796.
- Meschede, M., U. Asprion, and K. Reicherter. 1997. Visualization of tectonic structures in shallow-depth high-intensity ground penetrating radar (GPR) profiles. *Terra Nova* 9(4): 167-170.
- Molinda, G. M., W. D. Monaghan, G. L. Mowrey, and G. F. Persetic. 1996. Using ground penetrating radar for roof hazard detection in underground mines. USDOE. Pittsburgh Research Center, RI 9625.
- Nascimento da Silva, C. C., W. E. de Medeiros, E. F. Jarmin de Sa, and P. X. Neto. 2004. Resistivity and ground-penetrating radar images of fractures in a crystalline aquifer: a case study in Caicara farm – NE Brazil. *Journal of Applied Geophysics* 56: 295-307.
- Olhoeft, G. 1998. Electrical, magnetic, and geometric properties that determine ground penetrating radar performance. 177-182 pp. IN: Plumb, R. G. (ed.) *Proceedings of the Seventh International Conference on Ground-Penetrating Radar*. May 27 to 30, 1998, Lawrence, Kansas. Radar Systems and Remote Sensing Laboratory, University of Kansas.
- Pipan, M., L. Baradello, E. Forte, and A. Prizzon. 2000. GPR study of bedding planes, fractures and cavities in limestone. 682-687. IN: (Noon, D. Ed.) *Proceedings Eight International Conference on Ground-Penetrating Radar*. May 23 to 26, 2000, Goldcoast, Queensland, Australia. The University of Queensland.
- Porsani, J. L., V. R. Elis, and F. Y. Hiodo. 2005. Geophysical investigations for the characterization of fractured rock aquifer in Itu, SE Brazil. *Journal of Applied Geophysics* 57: 119-128.
- Singh, K. K. K. and R. K. S. Chauhan. 2002. Exploration of subsurface strata conditions for a limestone mining area in India with ground-penetrating radar. *Environmental Geology* 41: 966-971.
- Stevens, K. M., G. S. Lodha, A. L. Holloway, and N. M. Soonawala. 1995. The application of ground penetrating radar for mapping fractures in plutonic rocks within the Whiteshell Research Area, Pinawa, Manitoba, Canada. *Journal of Applied Geophysics*, 33: 125-141.
- Szerbiak, R. B., G. A. McMechan, R. Corbeanu, C. Forster, and S. H. Snelgrove. 2001. 3-D characterization of a clastic reservoir analog: from 3-D GPR data to a 3-D fluid permeability model. *Geophysics*, 66(4): 1026-1037.
- Toshioka, T., Tsuchida, T., and Sasahara, K., 1995, Application of GPR to detecting and mapping cracks in rock slopes: *Journal of Applied Geophysics*, v. 33, p. 119-124.
- Ulriksen, C. P. F. 1982. Application of impulse radar to civil engineering. Ph.D. dissertation. Lund University of Technology. Lund, Sweden.
- Wolock, D.M. Simulating the variable-source area concept of streamflow generation with the watershed model TOPMODEL. US Geological Survey. Water-Resources Investigation Report 93-4124.